Magnetic field induced quantum phase transition of the $S=\frac{1}{2}$ antiferromagnet K$_2$NaCrO$_8$

S. Nellutla,[1,][*] M. Pati,[2] Y.-J. Jo,[1] H. D. Zhou,[1] B. H. Moon,[3,4] D. M. Pajerowski,[3,4] Y. Yoshida,[3,4,][†] J. A. Janik,[1,5] L. Balicas,[1] Y. Lee,[3,4] M. W. Meisel,[3,4] Y. Takano,[3,4] C. R. Wiebe,[1,5,][‡] and N. S. Dalal[1,2]

[1]*National High Magnetic Field Laboratory, Tallahassee, Florida 32310, USA*
[2]*Department of Chemistry and Biochemistry, Florida State University, Tallahassee, Florida 32306, USA*
[3]*Department of Physics, University of Florida, Gainesville, Florida 32611-8440, USA*
[4]*National High Magnetic Field Laboratory, Gainesville, Florida 32611-8440, USA*
[5]*Department of Physics, Florida State University, Tallahassee, Florida 32310, USA*
(Received 8 December 2009; revised manuscript received 1 February 2010; published 24 February 2010)

The magnetic properties of alkali-metal peroxychromate K$_2$NaCrO$_8$ are governed by the $S=1/2$ pentavalent chromium cation, Cr^{5+}. Specific heat, magnetocalorimetry, ac magnetic susceptibility, torque magnetometry, and inelastic neutron-scattering data have been acquired over a wide range of temperature, down to 60 mK, and magnetic field, up to 18 T. The magnetic interactions are quasi-two-dimensional prior to long-range ordering, where $T_N=1.66$ K in $H=0$. In the $T\to0$ limit, the magnetic field tuned antiferromagnetic to spin-polarized phase transition suggests a critical field $\mu_oH_c=7.270$ T and a critical exponent $\alpha=0.481\pm0.004$. The neutron data indicate the magnetic interactions may extend over intraplanar nearest-neighbor and interplanar next-nearest-neighbor spins.

I. INTRODUCTION

The study of the similarities and differences between classical and quantum phase transitions has a rich history, and recent research has focused on systems in reduced dimensions.[1–4] For magnetic systems, the model Hamiltonian is often written as

$$\mathcal{H} = \sum_{(i,j)} J_{ij}\vec{S}_i \cdot \vec{S}_j + \vec{H} \cdot \overleftrightarrow{g} \cdot \sum_i \vec{S}_i, \qquad (1)$$

where the first sum over (i,j) is often restricted to nearest neighbor (nn) but may sometimes extend to include next-nearest neighbor (nnn), $J>0$ indicates antiferromagnetic interactions, and the Zeeman (second) term includes the presence of the externally applied magnetic field H and an anisotropic Landé g tensor. It is important to emphasize that both the spin and spatial dimensions are crucial elements of any model, and in this context, the critical exponents can be considered fingerprints for classifying the nature of the transition. In particular, the order parameter describing the transition can be characterized by $(T_c-T)^\beta$ as the temperature T approaches the critical temperature T_c or, in the $T\to0$ limit, by $(H_c-H)^\alpha$ for a quantum phase transition tuned by the magnetic field.[1–11]

The purpose of the present work was to consider the curious case of the pentavalent chromium cation, Cr^{5+}, an $S=1/2$ ($3d^1$) ion that is not a common choice for condensed-matter research.[12–20] Specifically, the alkali-metal peroxychromate K$_2$NaCrO$_8$ crystallizes with orthorhombic symmetry (space-group *Pbcm*) with the lattice parameters $a=8.5883$ Å, $b=7.9825$ Å, and $c=9.2432$ Å at 173 K.[14] The Cr^{5+} ion is bonded to four peroxy (O$_2$)$^{2-}$ ligands in a dodecahedral geometry, and the ions form the three-dimensional network shown in Fig. 1.[14,18] The data from EPR studies showed the g tensor is anisotropic, with $g_z=1.9851$, $g_y=1.9696$, and $g_x=1.9636$, the electronic ground state is d_{z^2}, and the magnetic z axis is along the [110]

crystal direction. During studies of the static magnetic susceptibility, $\chi_{dc}(\mu_oH=0.3$ T, $1.8\le T\le20$ K), and the specific heat, $C(0\le\mu_oH\le9$ T, $1.8\le T\le10$ K), Cage and Dalal[14] observed ordering signatures in polycrystalline samples. More specifically, while a rounded maximum was observed in $\chi_{dc}(\mu_oH=0.3$ T, $T\approx2.29$ K), the $C(\mu_oH\approx0$, $T\approx1.8$ K) data appeared to possess a λ-like peak. These signatures indicate the presence of low-dimensional antiferromagnetic behavior and the onset of long-range antiferromagnetic ordering. More recently, Choi *et al.*[18] performed low-temperature magnetization and ^{23}Na NMR measurements and identified a quantum phase transition from an antiferromagnetically ordered state to a spin-polarized state at critical field μ_oH_c of about 7.4 T, with $\beta=0.44\pm0.05$ in $\mu_oH=5$ T and $\beta=0.53\pm0.05$ in $\mu_oH=6.8$ T. Since mean-field theory yields $\beta=1/2$ for mag-
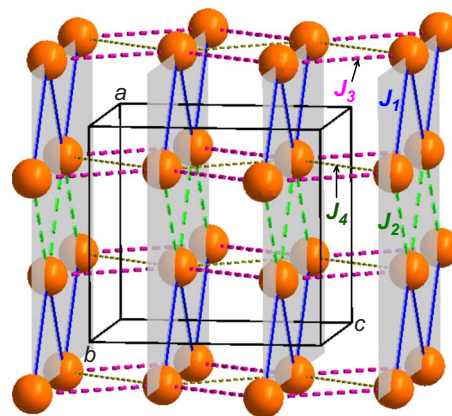

FIG. 1. (Color online) Spin network in K$_2$NaCrO$_8$ as seen along the b axis, where only the Cr^{5+} ions are shown for clarity. The vertical planes are the mirror planes containing J_1 (solid lines) and the J_2 (dashed lines) paths connecting the nn Cr^{5+} ions. Exchange paths corresponding to nnn interactions are labeled as J_3 (short-dashed lines) and J_4 (dotted lines).
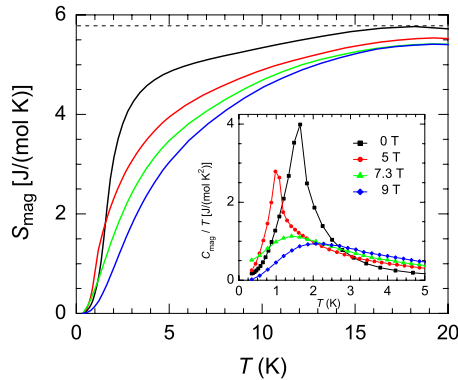
FIG. 2. (Color online) The temperature dependence of the magnetic entropy, $S_{mag}(T)$, at several representative magnetic fields. The inset shows the temperature dependence of the magnetic specific heat divided by temperature, $C_{mag}(T)/T$, at the same magnetic fields. $C_{mag}(T)$ was obtained by subtracting a lattice contribution from the total specific heat, see text. $S_{mag}(T)$ was obtained by integrating the data shown in the inset. As T increases, $S_{mag}(T)$ slowly approaches the $R \ln 2$ value, designated by the dashed line, as expected for a $S = 1/2$ system. In $H = 0$, about 60% of the entropy is acquired above T_N, indicating significant contributions from short-range correlations.

netization, these workers concluded that the high field magnetization of K_2NaCrO_8 is mean-field-like.

Herein, the results of specific heat, magnetocaloric effect, ac magnetic susceptibility, and torque magnetometry are reported to construct the magnetic phase diagram of K_2NaCrO_8, with particular emphasis on the $T \rightarrow 0$ limit of the magnetic field induced quantum phase transition. The data indicate the magnetic interactions are quasi-two-dimensional prior to long-range ordering. Inelastic neutron-scattering studies in zero magnetic field confirm the antiferromagnetic transition occurs without any low-temperature structural transitions and suggest the strongest magnetic interactions may include both nn and nnn ions. Furthermore, in the critical regime, the specific heat and magnetocaloric effect systematically identify the phase transition, while the magnetic measurements, although consistent with each other, yield a slightly shifted trend as $T \rightarrow 0$.

II. EXPERIMENTAL DETAILS

Single crystals of K_2NaCrO_8 were prepared by modification of the method of Riesenfeld.[12] The synthesis involves the reduction in Cr^{6+} by 30% H_2O_2 at 278 K in the 1:1 molar mixture of aqueous NaOH and KOH. Specific heat and magnetocaloric data were collected on single crystals with H applied along the c axis. The specific-heat studies employed the relaxation technique, 150 mK $\leq T \leq$ 20 K, with $\mu_o H \leq 18$ T using two different instruments. The magnetic specific heat, C_{mag}, was obtained by subtracting the zero-field Debye contribution, namely $C_{phonon} = (1.85 \times 10^{-3})T^3$ J/(mol K^4), from the total specific heat at all fields, and was integrated to yield the magnetic entropy, $S_{mag}(T)$ (Fig. 2). The magnetocaloric data, 150 mK $\leq T \leq$ 600 mK, were collected in $\mu_o H \leq 18$ T with
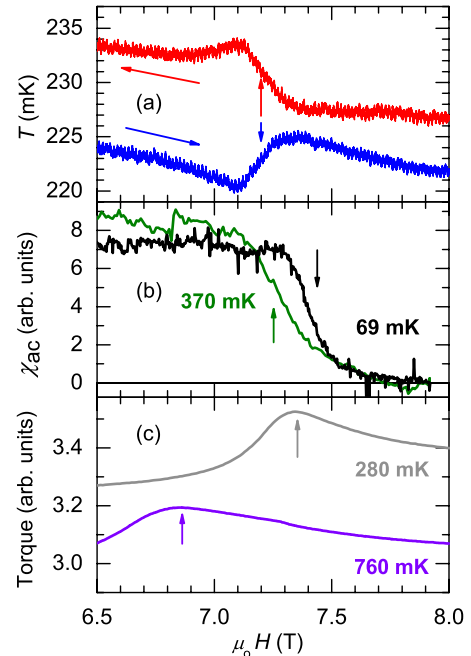

FIG. 3. (Color online) (a) The magnetocaloric effect curves for up and down field sweeps near 230 mK. (b) The ac susceptibility, $\chi_{ac}(H)$ at 69 and 370 mK. (c) The isothermal magnetic torque measured as a function of H. In each panel, the arrows designate the positions taken as the field induced phase transition.

a field sweep rate of 0.2 T/min [Fig. 3(a)]. For the ac susceptibility, χ_{ac}, a sample consisting of a random arrangement of microcrystallites (8.44 mg) was mounted, using GE varnish dissolved in ethanol, on a silver strip and wrapped in Kapton tape. The measurements were performed in a homemade dilution refrigerator probe using a standard set of inductively coupled coils operating at 1.114 kHz [Fig. 3(b)]. Torque magnetometry, performed down to 280 mK and up to 18 T, utilized a single crystal sample (1.2 mg) mounted using Stycast epoxy on a 0.005-in.-thick CuBe cantilever soldered to a post. The torque experienced by the sample deflects the cantilever, and the deflection was measured capacitively through a manual capacitance bridge excited at 30 V and 5 kHz [Fig. 3(c)]. Zero-field neutron-scattering work down to 1.4 K used a powderlike sample, generated by grinding microcrystals, that was mounted on the NIST-CNS disk chopper spectrometer (DCS) tuned to a wavelength of 4.8 Å.

III. EXPERIMENTAL RESULTS AND DISCUSSION

A. Specific heat and magnetocaloric effect

The distinct λ anomaly observed in the magnetic specific heat (Fig. 2) at $T_N = 1.66$ K and $H = 0$ indicates that K_2NaCrO_8 undergoes long-range antiferromagnetic ordering (LRAFO) as conjectured from earlier specific-heat measurements.[14] The LRAFO is suppressed in the presence of a magnetic field as T_N shifts slowly to lower temperatures until $\mu_o H$ reaches about 5 T and rapidly thereafter until the LRAFO is completely suppressed around 7.3 T. For $\mu_o H > 5$ T, the Schottky-type anomaly overlapping the
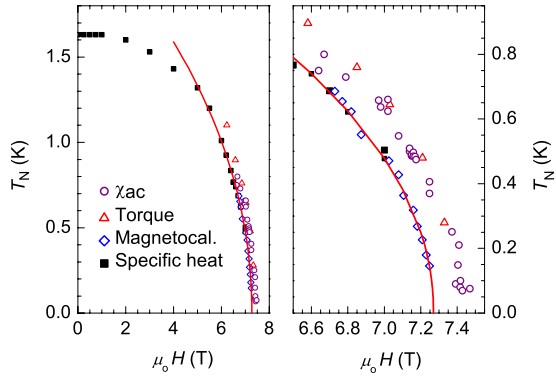
FIG. 4. (Color online) Magnetic phase diagram of K_2NaCrO_8. The solid line corresponds to Eq. (2) with $\mu_o H_c = 7.270$ T and $\alpha = 0.481 \pm 0.004$. The right panel provides an expanded view near $H_c(T \to 0)$, where the specific-heat and magnetocaloric transition points are systematically different than the ones extracted from standard analysis of the magnetic measurements, χ_{ac} and torque.

LRAFO at zero field becomes the dominant feature of $C_{mag}(T)$, and the corresponding position in temperature of the heat-capacity maximum shifts to higher temperatures. Consequently, the position of the phase transition is harder to identify. On the other hand, the magnetocaloric effect produces peaks in the up and down sweep directions, and these features correspond to the magnetic phase transition, while the center of these anomalies is identified as the transition point (Fig. 3). In Fig. 4, the transition points identified by these two methods are shown to yield a single trend of the phase boundary between the LRAFO and the spin-polarized state.

B. Magnetic susceptibility and torque

With respect to the magnetic studies using χ_{ac} and torque, the signatures designating the critical field of the transition are sharpest as $T \to 0$. For χ_{ac}, the inflection point between the low and high field regions is often used [Fig. 3(b)]. Alternatively, these data are integrated to yield the isothermal field dependence of the magnetization, $M(H)$, but an extrapolation protocol must be used as the location of the critical field is often smeared.[21–23] In our case, both routines provide essentially the same results that are plotted in Fig. 4. For the torque measurement, the peak of the response appears on a smooth, nearly quadratic background [Fig. 3(c)] and is taken as the location of the transition (Fig. 4). It is interesting to note that both techniques indicate a phase boundary that is slightly shifted from the one given by the specific-heat and magnetocaloric effect results, while the critical exponent remains the same within experimental uncertainty (Fig. 4). A detailed discussion of these observations is beyond the scope of this paper.

C. Magnetic phase diagram

Since the response of the specific heat unambiguously marks the transition and the magnetocaloric effect data identify the same critical field, these results were used to fit to
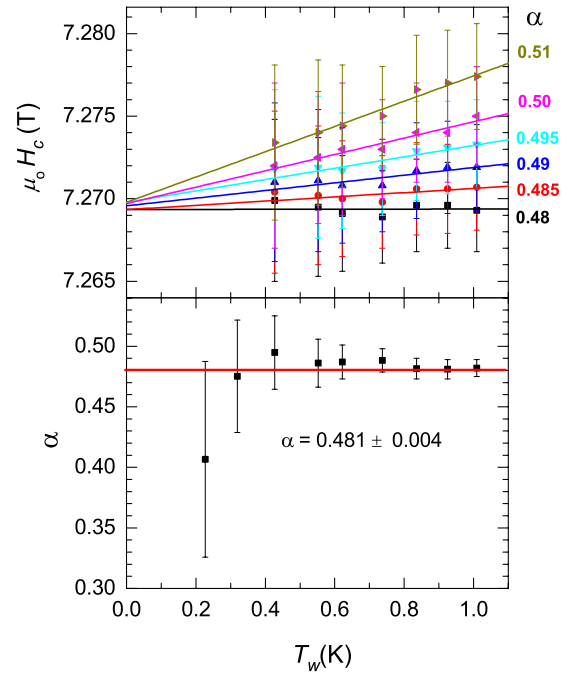

FIG. 5. (Color online) Estimates of (top panel) the critical field H_c and (bottom panel) the critical exponent α obtained from the "T-window" analysis of the transition, see text for detailed description. The results are $\mu_o H_c = 7.2696 \pm 0.0002$ T and $\alpha = 0.481 \pm 0.004$.

$$T_N = A(H_c - H)^\alpha. \qquad (2)$$

Care must be used when fitting Eq. (2), as both H_c and α need to be resolved.[7–11] Consequently, the "T-window" analysis and empirical convergence methods[8] were employed, by systematically varying the maximum temperature of the fits from 1 K to 230 mK, to extract the values of $\mu_o H_c = 7.270$ T and $\alpha = 0.481 \pm 0.004$. In detail, to extract H_c, the low-temperature ($T < 1$ K) phase boundary was fit to Eq. (2) for various α values in a temperature window, T_W, of decreasing size. For example, the phase boundary with a window size of 20 data points was fit to Eq. (2) with H_c and A as fitting parameters, while holding $\alpha = 0.48$. Then the window was successively reduced by removing the highest temperature point, and the fitting procedure was repeated. The resulting H_c values can then be plotted as a function of the upper limit of T_W (Fig. 5). The whole fitting procedure is then repeated for various fixed α values. The value of $\mu_o H_c = 7.2696 \pm 0.0002$ T was then obtained by taking a weighted average of the linearly extrapolated $H_c(T_W \to 0)$ values corresponding to various α values. This convergence of H_c to a single value allows a more precise determination of α than possible with a three parameter fit in which H_c, α, and A are simultaneous fitting parameters. The critical exponent α is then determined by following the same procedure, where the T-window analysis is performed when fixing $\mu_o H_c = 7.2696$ T (Fig. 5) and the result is $\alpha = 0.481 \pm 0.004$. Establishing the critical exponent of the transition begs the questions about the details of the network of magnetic interactions, so inelastic neutron-scattering experiments were performed.
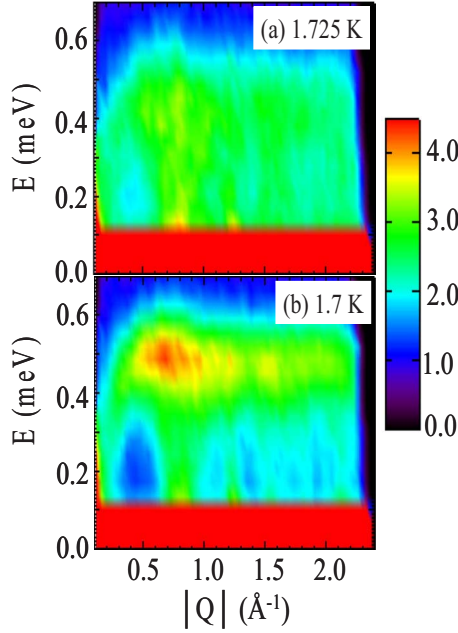
FIG. 6. (Color online) Inelastic neutron-scattering spectra at (a) 1.725 and (b) 1.7 K.

D. Neutron scattering

The neutron-scattering pattern at 1.725 K [Fig. 6(a)] reveals a magnetic excitation above $\Delta E = 0.2$ meV. After decreasing the temperature to 1.7 K [Fig. 6(b)], this excitation becomes sharper with a well-defined mode near $\Delta E = 0.5$ meV. When the magnetic excitations are summed over all Q, the broad peak near $\Delta E = 0.5$ meV sharpens for $T < 1.725$ K. The temperature dependence of the integrated area of the peak is consistent with the LRAFO observed in the zero-field specific heat.

Another noteworthy feature is that the excitation below the transition shows clear Q dependence, which has higher intensity at low Q. This magnetic contribution is consistent with an expression used to model the scattering from powders, where short-range isotropic spin correlations persist to the first few coordination shells of neighboring spins,[24] namely,

$$I(Q) \sim \sum_{i,j} \langle s_i s_j \rangle \frac{\sin(Qr_{i,j})}{Qr_{i,j}} \sim \frac{\sin(QR)}{QR}, \qquad (3)$$

where the final result is for the case of spins correlated over the nearest neighbors. Consequently, only one value R of r_{ij} (the distance between spins at sites i and j) is employed in our fitting procedure, where Eq. (3), multiplied by the magnetic form factor of the Cr^{5+} ion, has been used to fit to the net intensity shown in Fig. 7(a). This analysis yields $R = 6$ Å, which is close to the nn and nnn Cr⋯Cr distances that are in the range 5.8–6.2 Å. Ergo, the magnetic correlations are short range, extending over nn and nnn neighbors (Fig. 1). Furthermore, with decreasing temperature, the lattice Bragg peaks do not show obvious splitting or intensity change, thereby excluding the possibility of a structural change. On the other hand, new magnetic Bragg peaks with
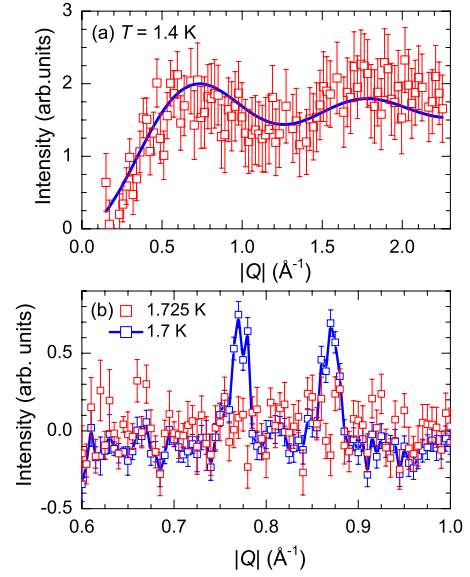

FIG. 7. (Color online) (a) A cut of the magnetic excitation near $\Delta E = 0.5$ meV at $T = 1.4$ K. The Q dependence of the intensity (open squares) is fit to Eq. (3) (solid line). (b) Appearance of the magnetic peaks at 1.7 K, after the data at 2 K have been subtracted as the lattice standard.

low intensity develop below 1.725 K [Fig. 7(b)] and are consistent with the ordering of a small moment at $T_N \approx 1.7$ K.

E. Structural considerations and magnetic interactions

Equipped with the result that short range magnetic interactions appear to extend over nn and nnn ions, the underlying network of these interactions can be re-examined. Previous theoretical and experimental studies established that although most of the unpaired electron density is on the Cr^{5+} ion, a significant portion of it can be found on the bound $(O_2)^{2-}$ ions.[25–28] Consequently, the potential superexchange pathways between Cr^{5+} ions in K_2NaCrO_8 can be expected to involve the $(O_2)^{2-}$, Na^+, and K^+ ions. Since the bond angle is an important factor in determining the ferromagnetic versus antiferromagnetic nature of the interactions,[29–31] the paths with larger O⋯Na/K⋯O angle are selected when more than one possible exchange pathway for a given Cr^{5+}⋯Cr^{5+} distance are present. This analysis leads to the results given in Table I, which tabulates the most influential exchange interactions between nn (the intraplanar J_1 and J_2)[18] and nnn (the interplanar J_3 and J_4) Cr^{5+} ions (Fig. 1). While the J_1 path involves Na^+ ions with a Na⋯O distance of ~2.4 Å and a bond angle ∠ONaO of 142°, the J_2 path involves K^+ ions with K⋯O distance of ~3.0 Å and an angle ∠OKO of 166°. The J_3 path involves Na^+ ions with a Na⋯O distance of ~2.4 Å and a bond angle ∠ONaO of 166° and the J_4 path involves K^+ ions with a K⋯O distance of ~2.6 Å and a bond angle ∠OKO of 131°.

All of the data suggest the intralayer interactions are somewhat stronger than the interlayer ones since the two-dimensional correlations develop before three-dimensional long-range order appears. Assuming a square lattice model,

TABLE I. Possible magnetic exchange pathways between Cr^{5+} ions in K_2NaCrO_8. The labels for the atoms are the same as used by Cage and Dalal (Ref. [14]) and the J_1 and J_2 designations are the same as used by Choi *et al.* (Ref. [18]).

Label	Cr⋯Cr (Å)	Pathway
J_1	5.837	O1⋯Na2⋯O2
J_2	5.888	O2⋯K1⋯O2
J_3	5.974	O6⋯Na2⋯O6
J_4	6.243	O3⋯K1⋯O3

the intraplanar exchange interaction, $J_{intra} \equiv (J_1+J_2)/2$, can be estimated from the data. For example, fitting $C_{mag}(T, \mu_o H = 18$ T$)$ yields $J_{intra} \sim 2.1$ K, whereas $H_c = 4J_{intra}/g\mu_B$ gives $J_{intra} \sim 2.4$ K. Both of these estimates are close to the value of 2.44 K obtained by fitting $\chi_{dc}(T)$ using a two-dimensional high-temperature series expansion.[14] A sense of the competition between the two-dimensional and three-dimensional interactions is further illustrated by the ratio $T_N/J_{intra} \sim 0.7$, which suggests that $J_{inter}/J_{intra} \sim 0.4$.[32] Obviously all indicators suggest that K_2NaCrO_8 possesses an "intermediate" dimensionality while the two-dimensional models still fit the data reasonably well, and this intriguing observation has been made previously in some Cu-based quasi-two-dimensional antiferromagnetic materials.[33] Finally, an aspect of the low magnetic field section of the phase diagram (Fig. 4) is noteworthy since T_N decreases with increasing field. This response contrasts with an increase in T_N observed in other quasi-two-dimensional systems where the magnetic field effectively induces anisotropy.[22,34]

IV. CONCLUSIONS

In summary, the low-temperature high magnetic field phase diagram of K_2NaCrO_8 has been established. In the $T \to 0$ limit, the magnetic field tuned antiferromagnetic to spin-polarized phase transition suggests a critical field $\mu_o H_c = 7.270$ T and a critical exponent $\alpha = 0.481 \pm 0.004$. The value of this critical exponent [Eq. (2)] depends on the universality class of the quantum phase transition, where $\alpha = 2/3$ is expected for Bose-Einstein condensation (BEC) (Refs. [1–4]) and $\alpha = 1/2$ is predicted for Ising-like spins.[2,10,35] The present data do not allow us to unambiguously differentiate between these two possible descriptions since a broad range of exponents is expected if the transition is not probed at sufficiently low temperatures.[7] The neutron data suggest the magnetic interactions extend over intraplanar nearest-neighbor and interplanar next-nearest-neighbor spins. For a deeper understanding of these results, especially the value of the critical exponent, inelastic neutron-scattering experiments should be performed on single crystals that are cooled to millikelvin temperatures in the presence of the magnetic field capable of spanning H_c. Fluctuation-induced heat release[36] and NMR (Ref. [37]) studies are alternatives that might provide decisive information.

*Present address: Department of Chemistry, North Carolina State University, Box 8204, Raleigh, North Carolina 27695.

†Present address: Institute of Applied Physics and Microstructure Research Center, University of Hamburg, D-20355 Hamburg, Germany.

‡Present address: Department of Chemistry, University of Winnipeg, Winnipeg, Canada, MB R3B 2E9.

[1] T. Giamarchi and A. M. Tsvelik, Phys. Rev. B **59**, 11398 (1999).

[2] S. Sachdev, *Quantum Phase Transitions* (Cambridge University Press, Cambridge, 1999).

[3] S. Sachdev, Nat. Phys. **4**, 173 (2008).

[4] T. Giamarchi, Ch. Rüegg, and O. Tchernyshyov, Nat. Phys. **4**, 198 (2008).

[5] M. Troyer, M. Imada, and K. Ueda, J. Phys. Soc. Jpn. **66**, 2957 (1997).

[6] S. Wessel, M. Olshanii, and S. Haas, Phys. Rev. Lett. **87**, 206407 (2001).

[7] O. Nohadani, S. Wessel, B. Normand, and S. Haas, Phys. Rev. B **69**, 220402(R) (2004).

[8] S. E. Sebastian, P. A. Sharma, M. Jaime, N. Harrison, V. Correa, L. Balicas, N. Kawashima, C. D. Batista, and I. R. Fisher, Phys. Rev. B **72**, 100404(R) (2005).

[9] T. Radu, H. Wilhelm, V. Yushankhai, D. Kovrizhin, R. Coldea, Z. Tylczynski, T. Lühmann, and F. Steglich, Phys. Rev. Lett. **95**, 127202 (2005).

[10] S. E. Sebastian, V. S. Zapf, N. Harrison, C. D. Batista, P. A. Sharma, M. Jaime, I. R. Fisher, and A. Lacerda, Phys. Rev. Lett. **96**, 189703 (2006).

[11] T. Radu, H. Wilhelm, V. Yushankhai, D. Kovrizhin, R. Coldea, Z. Tylczynski, T. Lühmann, and F. Steglich, Phys. Rev. Lett. **96**, 189704 (2006).

[12] E. H. Riesenfeld, Ber. Dtsch. Chem. Ges. **38**, 4068 (1905).

[13] M. H. Dickman and M. T. Pope, Chem. Rev. **94**, 569 (1994).

[14] B. Cage and N. S. Dalal, Chem. Mater. **13**, 880 (2001).

[15] E. Jimenez, P. Bonville, J. A. Hodges, P. C. M. Gubbens, J. Isasi, and R. Saez-Puche, J. Magn. Magn. Mater. **272-276**, 571 (2004).

[16] T. Nakajima, H. Mitamura, and Y. Ueda, J. Phys. Soc. Jpn. **75**,

054706 (2006).

[17] Y. Singh and D. C. Johnston, Phys. Rev. B **76**, 012407 (2007).

[18] K.-Y. Choi, S. Nellutla, A. P. Reyes, P. L. Kuhns, Y.-J. Jo, L. Balicas, H. Nojiri, M. Pati, and N. S. Dalal, Phys. Rev. B **78**, 214419 (2008).

[19] M. Kofu, J.-H. Kim, S. Ji, S.-H. Lee, H. Ueda, Y. Qiu, H.-J. Kang, M. A. Green, and Y. Ueda, Phys. Rev. Lett. **102**, 037206 (2009).

[20] M. Kofu, H. Ueda, H. Nojiri, Y. Oshima, T. Zenmoto, K. C. Rule, S. Gerischer, B. Lake, C. D. Batista, Y. Ueda, and S.-H. Lee, Phys. Rev. Lett. **102**, 177204 (2009).

[21] P. A. Goddard, J. Singleton, P. Sengupta, R. D. McDonald, T. Lancaster, S. J. Blundell, F. L. Pratt, S. Cox, N. Harrison, J. L. Manson, H. I. Southerland, and J. A. Schlueter, New J. Phys. **10**, 083025 (2008).

[22] F. Xiao, F. M. Woodward, C. P. Landee, M. M. Turnbull, C. Mielke, N. Harrison, T. Lancaster, S. J. Blundell, P. J. Baker, P. Babkevich, and F. L. Pratt, Phys. Rev. B **79**, 134412 (2009).

[23] A. Orendáčová, E. Čižmár, L. Sedláková, J. Hanko, M. Kajňaková, M. Orendáč, A. Feher, J. S. Xia, L. Yin, D. M. Pajerowski, M. W. Meisel, V. Zeleňák, S. Zvyagin, and J. Wosnitza, Phys. Rev. B **80**, 144418 (2009).

[24] E. F. Bertaut and P. Burlet, Solid State Commun. **5**, 279 (1967).

[25] B. R. McGarvey, J. Chem. Phys. **37**, 2001 (1962).

[26] N. S. Dalal, J. M. Millar, M. S. Jagadeesh, and M. S. Seehra, J. Chem. Phys. **74**, 1916 (1981).

[27] B. Cage, A. K. Hassan, L. Pardi, J. Krzystek, L.-C. Brunel, and N. S. Dalal, J. Magn. Reson. **124**, 495 (1997).

[28] M. Roch, J. Weber, and A. F. Williams, Inorg. Chem. **23**, 4571 (1984).

[29] P. W. Anderson, in *Solid State Physics*, edited by F. Seitz and D. Turnbull (Academic Press, New York, 1963), Vol. 14, p. 99.

[30] J. B. Goodenough, *Magnetism and the Chemical Bond* (Wiley and Sons, New York, 1963).

[31] P. J. Hay, J. C. Thibeault, and R. Hoffmann, J. Am. Chem. Soc. **97**, 4884 (1975).

[32] C. Yasuda, S. Todo, K. Hukushima, F. Alet, M. Keller, M. Troyer, and H. Takayama, Phys. Rev. Lett. **94**, 217201 (2005).

[33] F. M. Woodward, A. S. Albrecht, C. M. Wynn, C. P. Landee, and M. M. Turnbull, Phys. Rev. B **65**, 144412 (2002).

[34] P. Sengupta, C. D. Batista, R. D. McDonald, S. Cox, J. Singleton, L. Huang, T. P. Papageorgiou, O. Ignatchik, T. Herrmannsdörfer, J. L. Manson, J. A. Schlueter, K. A. Funk, and J. Wosnitza, Phys. Rev. B **79**, 060409(R) (2009).

[35] C. J. Hamer, J. Oitmaa, Z. Weihong, and R. H. McKenzie, Phys. Rev. B **74**, 060402(R) (2006).

[36] Y. H. Kim, N. Kaur, B. M. Atkins, N. S. Dalal, and Y. Takano, Phys. Rev. Lett. **103**, 247201 (2009).

[37] S. Suh, K. A. Al-Hassanieh, E. C. Samulon, J. S. Brooks, W. G. Clark, P. L. Kuhns, L. L. Lumata, A. Reyes, I. R. Fisher, S. E. Brown, and C. D. Batista, arXiv:0905.0718 (unpublished).